

RESEARCH

Open Access



Changes in the microstructure of compact and trabecular bone tissues of mice subchronically exposed to alcohol

Monika Martiniakova¹, Anna Sarocka¹, Ramona Babosova¹, Birgit Grosskopf^{2*}, Edyta Kapusta³, Zofia Goc³, Grzegorz Formicki³ and Radoslav Omelka⁴

Abstract

Background: Alcohol is one of the most commonly consumed neurotoxins by humans. Its negative effect on bone health is known for a long time. However, its impact on qualitative and quantitative 2D characteristics of the compact bone is still unclear. Therefore, the aim of this study was to investigate in detail the effects of subchronic alcohol exposure on compact and trabecular bone tissues microstructure of laboratory mice using 2D and 3D imaging methods. Ten clinically healthy 12 weeks-old mice (males) were randomly divided into two groups. Animals from experimental group (group E; n = 5) drank a solution composed of 15% ethanol and water (1.7 g 100% ethanol kg⁻¹ b.w. per day) for 8 weeks, while those from control group (group C; n = 5) drank only water.

Results: Subchronic exposure to alcohol leads to several changes in qualitative 2D characteristics of the compact bone such as the presence of primary vascular radial bone tissue in *pars anterior* of endosteal border and a higher number of resorption lacunae (five times more) in the middle part of *substantia compacta*. Morphometrical 2D evaluations of the compact bone showed significantly increased sizes of primary osteons' vascular canals ($p < 0.05$) in mice from the experimental group (E group). Sizes of Haversian canals and secondary osteons were not affected by alcohol consumption. In mice from the E group, significantly lower values for relative bone volume and bone mineral density of the compact bone were observed. In the trabecular bone, decreased values for bone volume, trabecular number, trabecular thickness and bone surface ($p < 0.05$) were documented.

Conclusions: Alcohol decreased not only bone volume and density of the compact bone, but it also reduced trabecular bone volume and leads to trabecular thinning. It caused vasodilation of primary osteons' vascular canals and increased porosity in the compact bone.

Keywords: Alcohol, Microstructure, Compact bone, Trabecular bone, Mice

Background

Bone is highly hierarchical in structure, and therefore, any study of its structure and properties must investigate the tissue at several levels of organization in order to gain a complete understanding of the influence of structure and composition on these properties [1]. The extracellular matrix, and especially connective tissue with its collagen (represents more than 90% of the organic bone

matrix) confers resistance to the structure and establishes the biomechanical properties of the tissue [2]. Bone mineral (mostly hydroxyapatite) provides mechanical rigidity and load-bearing strength to bone [3]. The relation between organic and non-organic part is crucial for the bone quality [1, 2].

Alcohol consumption is well known to be a lifestyle factor that markedly increases the risk of osteoporosis [4], osteomalacia, aseptic necrosis (primarily necrosis of the femoral head) [5] and fracture incidence [6]. These pathologies are based on the frequent finding of a low bone mass, decreased bone mineral content (BMC) and

*Correspondence: birgit.grosskopf@biologie.uni-goettingen.de

² Institute of Zoology and Anthropology, Georg-August University, 37073 Göttingen, Germany

Full list of author information is available at the end of the article



bone mineral density (BMD) [7]. In addition, the consumption of alcohol disrupts compact and trabecular bone microarchitecture. In general, alcohol negatively affects bone structure for several reasons. Bone remodeling is modified, mostly due to a decreased bone formation [8]. According to Broulik et al. [9], an inhibited bone formation, bone repair and decreased bone strength were identified in rats fed ethanol (7.6 g of 95% ethanol kg^{-1} b.w. daily for 3 months). Also, chronic alcohol abuse caused changes in calcium regulating hormones, mineral homeostasis, mechanical loading [10] and led to an accumulation of reactive oxygen species (ROS) [11]. Furthermore, NADPH oxidase expression was upregulated in osteoblasts of rats infused intragastrically with ethanol-containing liquid diets (12 g ethanol kg^{-1} daily for 4 weeks) [12]. These effects of alcohol may be caused by its high caloric density and bioactive properties [13]. Although alcohol belongs to the most commonly consumed neurotoxins by humans, there are no studies describing its influence on qualitative and quantitative 2D characteristics of the compact bone. Therefore, our study was aimed to determine in detail the microstructure of compact and trabecular bone tissues of mice after a subchronic peroral exposure to alcohol using 2D and 3D imaging methods.

Methods

Animals

In our experiment, ten clinically healthy 12-week-old Swiss mice (males) were used. The animals were obtained from the accredited experimental laboratory of the Pedagogical University in Cracow. The mice were randomly divided into two groups, of five animals each and were housed in individual flat-deck wire cages under a constant photoperiod of 12 h of daylight, temperature 20–24 °C and humidity 55% \pm 10%. In the experimental group (group E) mice received a solution composed of 15% ethanol and water (1.7 g 100% ethanol kg^{-1} b.w. per day) for 8 weeks. The solution of alcohol in water has been made every day and it was administered orally to mice by a syringe (six doses of 50 μl 15% ethanol daily). Therefore, we have known the exact amount of daily fluid alcohol consumption. This corresponds to a consumption of six 0.5 dl of 40% ethanol or 2.5 l of 12° beer for 75 kg male adults. The second group without alcohol administration served as a control (group C).

Procedures

At the end of treatment period, mice were put into a state of deep anesthesia by Vetbutal (Biowet, Poland) administration in the amount of 35 mg kg^{-1} b.w. and

their femora were used for microscopical analyses. Each femur was macerated, degreased and embedded in epoxy resin Biodur (Günter von Hagens, Heidelberg, Germany) according to the methodology of Martiniakova et al. [14]. Transverse thin sections (70–80 μm) were prepared with a sawing microtome (Leitz 1600, Leica, Wetzlar, Germany) and affixed to glass slides with Eukitt (Merck, Darmstadt, Germany) [15]. The qualitative characteristics of the compact bone (2D analysis) were determined according to the internationally accepted classification systems of Enlow and Brown [16] and Ricqles et al. [17]. The quantitative parameters of the compact bone (2D analysis) were assessed using software Motic Images Plus 2.0 ML (Motic China Group Co., Ltd.) in all sides (*anterior*, *posterior*, *medialis*, *lateralis*) of thin sections. We measured area (μm^2), perimeter (μm), maximum and minimum diameters (μm) of the primary osteons' vascular canals, Haversian canals and secondary osteons in all sides of thin section in order to minimize statistical differences in the individual. Secondary osteons were distinguished from primary osteons (i.e., primary vascular canals) on the basis of the well-defined peripheral boundary (cement line) between secondary osteons and surrounding tissue. Cement line delimits secondary osteons and also Haversian canals and it is not found in primary osteons. In addition, secondary osteons intersect circumferential lamellae, whereas primary osteons do not [14, 17–19].

Quantitative 3D analyses of compact and trabecular bone tissues were determined using microcomputed tomography (μCT 50, Scanco Medical). Compact bone structure was analysed in a region of interest starting 5.2 mm from the end of the growth plate (distal epiphysis) and extending 1.5 mm at femoral midshaft. Following parameters were measured: relative bone volume (%), bone mineral density (BMD) (mg HA cm^{-3}), relative bone volume without marrow cavity (%), bone surface without marrow cavity (mm^2) and cortical bone thickness (mm). Trabecular bone structure was analysed in a region of interest starting 1.2 mm from the end of the growth plate (distal epiphysis) and extending 1.5 mm. We measured relative bone volume (%), trabecular number (mm^{-1}), trabecular thickness (mm), trabecular separation (mm) and bone surface (mm^2).

Statistics

The measured values were expressed as mean \pm standard deviation. The differences in quantitative characteristics of compact and trabecular bone tissues between mice from E and C groups were determined using an unpaired t-test ($p < 0.05$).

Results

Qualitative 2D analysis of compact bone tissue

The femora of mice from the C group had the following compact bone microstructure in common. The endosteal border consisted of a zone of non-vascular bone tissue (mainly in *anterior*, *medialis* and *lateralis* sides). This tissue included cellular lamellae and osteocytes. Also, primary vascular radial bone tissue (contained branching or non-branching vascular canals radiating from the marrow cavity) was observed in *pars posterior* of endosteal surface. In the middle part of the compact bone (in *anterior*, *lateralis* and *posterior* sides), irregular Haversian bone tissue was identified. This tissue consisted of Haversian systems (secondary osteons) which were scattered, isolated and relatively few in number. In addition, few resorption lacunae were found in *pars anterior*. Non-vascular bone tissue was observed in *pars medialis* of the central area of bone. Finally, the periosteal surface was formed by non-vascular bone tissue (Fig. 1a).

Mice from the E group displayed differences in *substantia compacta* compared to those from the C group (Fig. 1b). *Pars anterior* of the endosteal border was also formed by primary vascular radial bone tissue (not only by non-vascular bone tissue). Furthermore, more resorption lacunae (five times more) were identified in the middle part of *substantia compacta* (in *pars anterior* and *lateralis*).

Quantitative 2D analysis of compact bone tissue

Altogether, 314 primary osteons' vascular canals, 56 Haversian canals and 56 secondary osteons were measured in mice from both groups. The results are summarized in Table 1. We have found that all measured variables (area, perimeter, maximal and minimal diameters) of the primary osteons' vascular canals had significantly higher values ($p < 0.05$) in mice from the E group. On the other hand, sizes of Haversian canals and secondary osteons did not differ significantly between mice from the E and C groups.

Quantitative 3D analysis of compact bone tissue

The values for relative bone volume and BMD were significantly decreased in mice from the group E. On the other hand, insignificant effects of subchronic alcohol consumption on relative bone volume without marrow cavity, bone surface and cortical bone thickness were observed. The results are summarized in Table 2. Representative reconstructed 3D images of the compact bone are illustrated in Fig. 2a, b.

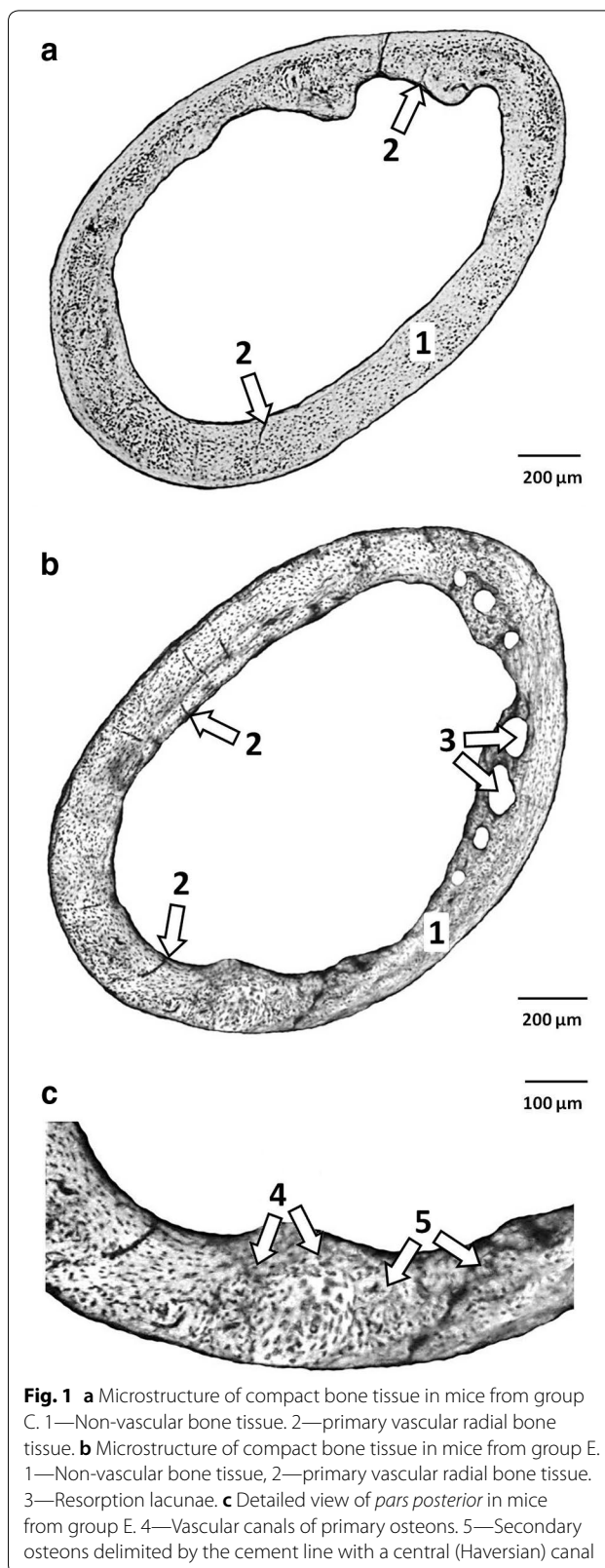


Fig. 1 a Microstructure of compact bone tissue in mice from group C. 1—Non-vascular bone tissue. 2—primary vascular radial bone tissue. b Microstructure of compact bone tissue in mice from group E. 1—Non-vascular bone tissue, 2—primary vascular radial bone tissue. 3—Resorption lacunae. c Detailed view of *pars posterior* in mice from group E. 4—Vascular canals of primary osteons. 5—Secondary osteons delimited by the cement line with a central (Haversian) canal

Table 1 Data of quantitative 2D analysis of compact bone tissue in mice from both groups

	Group	N	Area (μm^2)	Perimeter (μm)	Max. diameter (μm)	Min. diameter (μm)
Primary osteons' vascular canals	C	165	20.4533 \pm 3.41	16.06 \pm 1.355	2.6564 \pm 0.296	2.402 \pm 0.226
	E	149	30.1013 \pm 6.14	19.496 \pm 2.033	3.2987 \pm 0.404	2.876 \pm 0.362
	t-test		$p < 0.05$	$p < 0.05$	$p < 0.05$	$p < 0.05$
Haversian canals	C	26	22.06 \pm 3.42	16.73 \pm 1.32	2.81 \pm 0.28	2.46 \pm 0.27
	E	30	22.20 \pm 4.86	16.65 \pm 1.85	2.72 \pm 0.36	2.54 \pm 0.30
	t-test		NS	NS	NS	NS
Secondary osteons	C	26	243.63 \pm 37.63	55.48 \pm 4.47	9.38 \pm 0.89	8.23 \pm 0.64
	E	30	245.41 \pm 48.99	55.71 \pm 5.64	9.54 \pm 1.09	8.14 \pm 0.83
	t-test		NS	NS	NS	NS

N number of measured structures, NS non-significant differences

Table 2 Data of quantitative 3D analysis of compact bone tissue in mice from both groups

Group	N	BV/TV (%)	BMD (mg HA cm^{-3})	BV/TV* (%)	Bs. (mm^2)	Ct.Th. (mm)
C	5	0.509 \pm 0.016	577.448 \pm 27.439	0.958 \pm 0.014	5.456 \pm 1.356	0.195 \pm 0.014
E	5	0.449 \pm 0.022	513.406 \pm 37.514	0.957 \pm 0.003	4.704 \pm 0.753	0.175 \pm 0.010
t-test		$p < 0.05$	$p < 0.05$	NS	NS	NS

n number of measurements, NS non-significant differences, BV/TV relative bone volume, BMD bone mineral density, BV/TV* relative bone volume without marrow cavity, Bs. bone surface, Ct.Th. cortical bone thickness

Quantitative 3D analysis of trabecular bone tissue

The values for relative bone volume, trabecular number, trabecular thickness and bone surface were significantly decreased ($p < 0.05$) in mice from the E group. On the contrary, the value for trabecular separation was significantly increased in these mice. The results are summarized in Table 3. Representative reconstructed 3D images of the trabecular bone are illustrated in Fig. 2c, d.

Discussion

The results of qualitative 2D analysis of the compact bone in mice from the C group are consistent with those of other researchers [16, 20, 21]. However, subchronic exposure to ethanol leads to several changes such as the presence of primary vascular radial bone tissue in *pars anterior* of endosteal border and a higher number of resorption lacunae (increased porosity) in the middle part of *substantia compacta*. These differences can be caused by inhibition of periosteal and endosteal bone formation due to alcohol administration [22]. The results by Rocco et al. [23] showed that alcohol metabolized by CYP2E1 is responsible for a formation of reactive oxygen species (ROS), such as hydrogen peroxide and superoxide ions which enhance bone resorption [24] and osteoclastogenesis [25]. During growth, the entire bone is moved and repositioned in a progressive anterior direction [26]. Also, this bone region is characteristic by a higher degree

of mineralization [27]. According to Sivaraj and Adams [28], vascularization constitutes the first phase of ossification: the blood vessels invade the cartilage and later produce resorption via the osteoclasts originating from the nearby vessels. In the same way, vascular neof ormation is the first event in the repair of fractures or bone regeneration.

Our results also revealed significantly increased sizes of primary osteons' vascular canals in mice from the E group. Primary osteons' vascular canals contain blood vessels which provide nutrition for the bone [29]. Pries et al. [30] showed that blood vessels can adapt its structure (vascular remodeling) in response to continuous functional changes. Vasodilation of these vascular canals in mice exposed to alcohol could be associated with deleterious effect of alcohol on blood vessels. According to Palaparthy [31], alcohol has a significant effect on cardiovascular system including peripheral vasodilation. Generally, angiogenesis is regulated by various factors, including signaling through vascular endothelial growth factor (VEGF) receptors [32]. In general, hypoxia can be originated by the presence of alcohol in the liver [33]. Hypoxic conditions can also potently stimulate a formation of an extensive vascular network [34]. On the other hand, non-significant changes in the size of Haversian canals (which also contain blood vessels) were observed in mice from E group. It is generally known that the structure of primary and secondary osteons is different. Haversian canals are surrounded by a cement line which

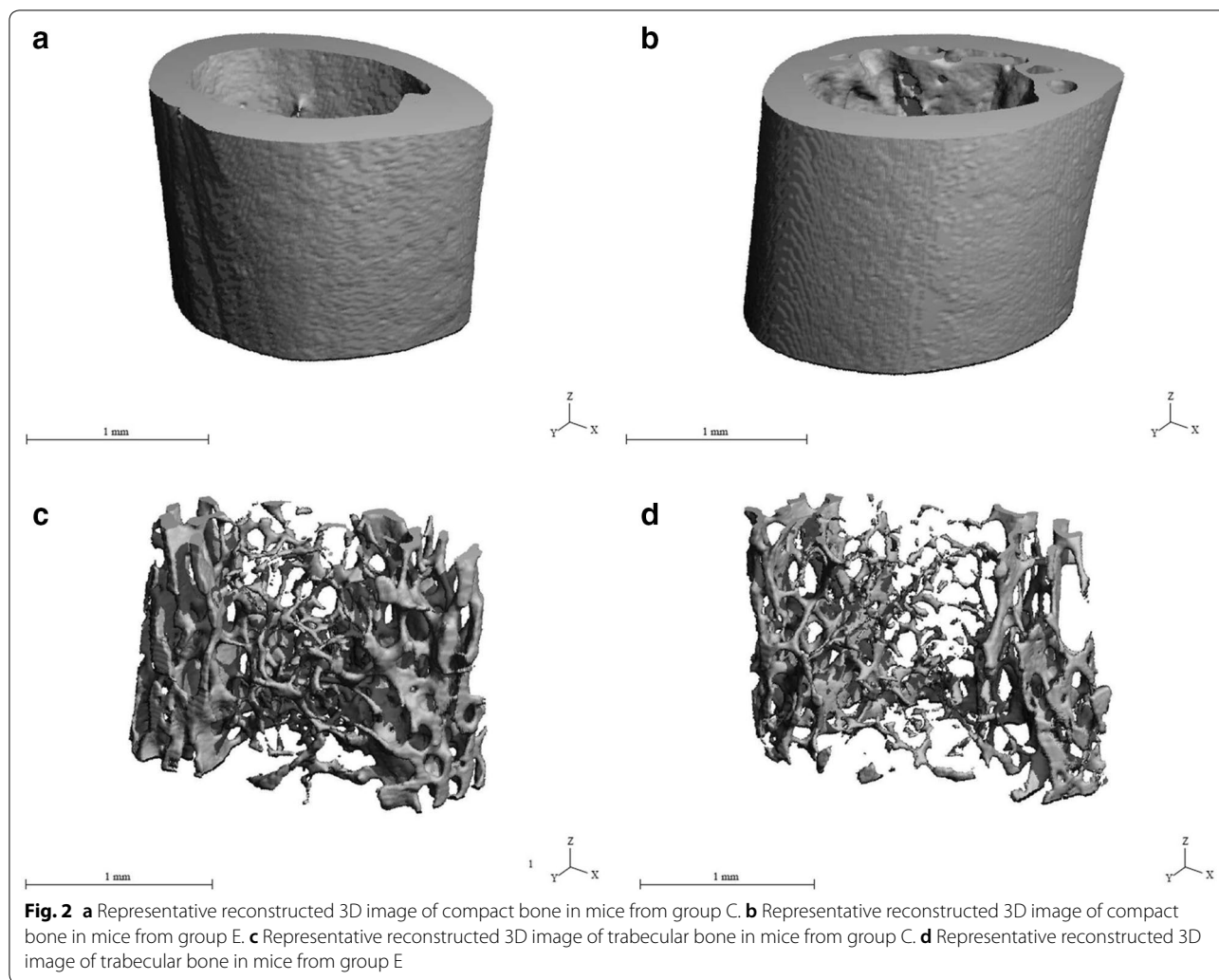


Table 3 Data of quantitative 3D analysis of trabecular bone tissue in mice from both groups

Group	N	BV/TV (%)	Tb.N. (mm ⁻¹)	Tb.Th. (mm)	Tb.Sp. (mm)	Bs. (mm ²)
C	5	0.158 ± 0.010	4.616 ± 0.034	0.047 ± 0.001	0.210 ± 0.002	20.429 ± 3.516
E	5	0.078 ± 0.006	3.919 ± 0.134	0.035 ± 0.001	0.253 ± 0.011	13.417 ± 0.872
t-test		<i>p</i> < 0.05	<i>p</i> < 0.05	<i>p</i> < 0.05	<i>p</i> < 0.05	<i>p</i> < 0.05

n number of measurements, *BV/TV* relative bone volume, *Tb.N.* trabecular number, *Tb.Th.* trabecular thickness, *Tb.Sp.* trabecular separation, *Bs.* bone surface

is not found in primary osteons [14, 17–19]. We suppose that the cement line is a main reason for different results in histomorphometry of both canals.

Quantitative 3D analysis of the compact bone discovered significantly lower values for relative bone volume and BMD in mice administered alcohol. Decreased BMD and relative bone volume were also documented in other studies with alcohol-fed mice (36% ethanol Lieber-DeCarli diet for 78 days) [35] and rats (35% ethanol

Lieber-DeCarli liquid diet for 42 days) [36]. According to Wezeman et al. [37], chronic alcohol exposure can stimulate metabolism of adipocytes resulting in triglyceride accumulation in diaphyseal marrow of the bone. Also, other cellular changes in the bone marrow and endocortical surface of the bone caused by alcohol consumption lead to the disruption of bone remodeling involving reduction of the number and activity of basic multicellular units [6]. Therefore, decreased bone formation rate

followed by a low bone mass and a decreased BMD are generally identified in alcoholics.

We found significantly decreased values for relative bone volume, trabecular number, trabecular thickness and bone surface in mice from the E group. These results confirmed the literature [38–40] showing that alcohol intake reduces the trabecular bone volume and leads to trabecular thinning. According to Turner et al. [41], alcohol also impairs the effects of growth hormone (an important physiological regulator of bone growth) on tibial growth and trabecular bone formation. Furthermore, alcohol decreases concentration of leptin [39]. Leptin has a direct anabolic effect on the bone that leads to the decline of osteoblastic differentiation [42]. Therefore, evident changes in morphometry of the trabecular bone could be associated with these aspects.

In summary, alcohol decreased not only bone volume and density of the compact bone, but it also reduced trabecular bone volume and leads to trabecular thinning in our male mice. In men, chronic heavy alcohol consumption also decreased BMD in different skeletal sites, including femur [7, 43, 44]. Also, decreased cortical thickness, trabecular thickness and volume were identified in black male patients suffering from alcohol-induced bone disease and pancreatitis [45]. Vasodilation of primary osteons' vascular canals and increased porosity in the compact bone were observed in male mice. In general, bone microstructure of adult humans is composed mainly of dense Haversian bone tissue with a quite dense concentration of secondary osteons. Primary osteons are only occasionally found in the bones [19, 46]. Therefore, the information about vasodilation of primary osteons' vascular canals in human alcoholics is still absent. Increased porosity (including increased bone resorption parameters) was also identified in osteoporotic males [47]. Heavy alcohol consumption is known to induce secondary osteoporosis in both females and males. It follows that almost all changes described in our study are observed in humans consuming alcohol.

Conclusions

Subchronic peroral exposure to alcohol at the dose used in our study affected both compact and trabecular bone tissues microstructure. In the compact bone, increased porosity, significantly higher values for primary osteons' vascular canals and decreased values for relative bone volume and bone mineral density were identified. In the trabecular bone, decreased values for bone volume, trabecular number, trabecular thickness and bone surface were documented. Our study supports previously published results showing that excess alcohol consumption is damaging for both compact and trabecular bone tissues. However, it provides the first information related to

changes in qualitative and quantitative 2D characteristics of the compact bone of mice subchronically exposed to ethanol.

Abbreviations

BMC: bone mineral content; BMD: bone mineral density; b.w.: body weight; g: gram; kg: kilogram; ROS: reactive oxygen species; NADPH: nicotinamide adenine dinucleotide phosphate; μm : micrometre; μCT : microcomputed tomography; BV/TV: relative bone volume; BV/TV^{*}: relative bone volume without marrow cavity; Bs.: bone surface without marrow cavity; Ct.Th.: cortical bone thickness; HA: hydroxyapatite; Tb.N.: trabecular number; Tb.Sp.: trabecular separation; Tb.Th.: trabecular thickness; mm: millimetre; N: number of measurements; CYP2E1: cytochrome P450 2E1; VEGF: vascular endothelial growth factor; NS: non-significant differences; SD: standard deviation.

Authors' contributions

MM was responsible for quantitative 3D analysis of the trabecular bone and writing the article. AS was responsible for quantitative 2D analysis of the compact bone and helped with writing the article. RB was responsible for qualitative 2D analysis of the compact bone. BG was responsible for preparation of histological sections and corresponds with co-authors. EK was responsible for quantitative 3D analysis of the compact bone. ZG was responsible for animal care and sampling of femora. GF conceived and designed the research. RO was responsible for photodocumentation of histological sections and statistical analyses. All authors read and approved the final manuscript.

Author details

¹ Department of Zoology and Anthropology, Constantine the Philosopher University in Nitra, 949 74 Nitra, Slovakia. ² Institute of Zoology and Anthropology, Georg-August University, 37 073 Göttingen, Germany. ³ Department of Animal Physiology and Toxicology, Pedagogical University of Cracow, 30 084 Cracow, Poland. ⁴ Department of Botany and Genetics, Constantine the Philosopher University in Nitra, 949 74 Nitra, Slovakia.

Competing interests

The authors declare that they have no competing interests.

Availability of data and materials

The datasets supporting the conclusions of this article are included within the article. The raw data can be requested from the corresponding author.

Consent for publication

Not applicable.

Ethics approval and consent to participate

All the applied procedures were approved by the First Local Ethic Committee on Experiments on Animals in Cracow (Resolution Number 175/2012).

Funding

This work was supported by the Slovak Research and Development Agency under the contract No. SK-PL-2015-0032. The study was also supported by the projects VEGA 1/0653/16 and KEGA 031UKF-4/2016.

Publisher's Note

Springer Nature remains neutral with regard to jurisdictional claims in published maps and institutional affiliations.

Received: 12 September 2017 Accepted: 18 May 2018

Published online: 24 May 2018

References

1. Tzaphlidou M. Bone architecture: collagen structure and calcium/phosphorus maps. *J Biol Phys.* 2008;34:39–49.
2. Berillis P, Emfietzoglou D, Tzaphlidou M. Collagen fibril diameter in relation to bone site and to calcium/phosphorus ratio. *Sci World J.* 2006;6:1109–13.

3. Landis WJ. The strength of a calcified tissue depends in part on the molecular structure and organization of its constituent mineral crystals in their organic matrix. *Bone*. 1995;16:533–44.
4. Seeman E. *Osteoporosis*. 2nd ed. San Diego: Academic Press; 2001.
5. González-Reimers E, Quintero-Platt G, Rodríguez-Rodríguez E, Martínez-Riera A, Alvisa-Negrín J, Santolaria-Fernández F. Bone changes in alcoholic liver disease. *World J Hepatol*. 2015;7:1258–64.
6. Chakkalakal DA. Alcohol-induced bone loss and deficient bone repair. *Alcohol Clin Exp Res*. 2005;29:2077–90.
7. Turner RT. Skeletal response to alcohol. *Alcohol Clin Exp Res*. 2000;24:1693–701.
8. Maurel DB, Boisseau N, Pallu S, Rochefort GY, Benhamou CL, Jaffre C. Regular exercise limits alcohol effects on trabecular, cortical thickness and porosity, and osteocyte apoptosis in the rat. *Joint Bone Spine*. 2013;80:492–8.
9. Broulik PD, Vondrová J, Růžicka P, Sedláček R, Zima T. The effect of chronic alcohol administration on bone mineral content and bone strength in male rats. *Physiol Res*. 2010;59:599–604.
10. Bartlett PJ, Antony AN, Agarwal A, Hilly M, Prince VL, Combettes L, et al. Chronic alcohol feeding potentiates hormone-induced calcium signaling in hepatocytes. *J Physiol*. 2017;595:3143–64.
11. Park BJ, Lee YJ, Lee HR. Chronic liver inflammation: clinical implications beyond alcoholic liver disease. *World J Gastroenterol*. 2014;20:2168–75.
12. Chen JR, Lazarenko OP, Shankar K, Blackburn ML, Lumpkin CK, Badger TM, et al. Inhibition of NADPH oxidases prevents chronic ethanol-induced bone loss in female rats. *J Pharmacol Exp Ther*. 2011;336:734–42.
13. Nielsen SJ, Kit BK, Fakhouri T, Ogden CL. Calories consumed from alcoholic beverages by US adults 2007–2010. NCHS Data Brief, vol. 110. Hyattsville: US Department of Health and Human Services, Centers for disease control and prevention, National Center for Health Statistics; 2012. p. 1–8.
14. Martiniaková M, Omelka R, Grosskopf B, Sirotkin AV, Chrenek P. Sex-related variation in compact bone microstructure of the femoral diaphysis in juvenile rabbits. *Acta Vet Scand*. 2008;50:15.
15. Martiniaková M, Omelka R, Jancová A, Stawarz R, Formicki G. Heavy metal content in the femora of yellow-necked mouse (*Apodemus flavicollis*) and wood mouse (*Apodemus sylvaticus*) from different types of polluted environment in Slovakia. *Environ Monit Assess*. 2010;171:651–60.
16. Enlow DH, Brown SO. A comparative histological study of fossil and recent bone tissues. Part I. *Texas J Sci*. 1956;8:405–12.
17. de Ricqlès AJ, Meunier FJ, Castanet J, Francillon-Vieillot H. Comparative microstructure of bone. In: Hall BK, editor. *Bone*, vol. 3., Bone matrix and bone specific products. Boca Raton: CRC Press; 1991. p. 1–78.
18. Martiniaková M, Boboňová I, Omelka R, Grosskopf B, Stawarz R, Toman R. Structural changes in femoral bone tissue of rats after subchronic peroral exposure to selenium. *Acta Vet Scand*. 2013;55:8.
19. Brits D, Steyn M, L'Abbé EN. A histomorphological analysis of human and non-human femora. *Int J Legal Med*. 2014;128:369–77.
20. Treuting PM, Dintzis SM, Montine KS. *Comparative anatomy and histology: a mouse, rat, and human atlas*. 2nd ed. Oxford: Academic Press; 2017.
21. Reim NS, Breig B, Stahr K, Eberle J, Hoeflich A, Wolf E, et al. Cortical bone loss in androgen-deficient aged male rats is mainly caused by increased endocortical bone remodeling. *J Bone Miner Res*. 2008;23:694–704.
22. Hefferan TE, Kennedy AM, Evans GL, Turner RT. Disuse exaggerates the detrimental effects of alcohol on cortical bone. *Alcohol Clin Exp Res*. 2003;27:111–7.
23. Rocco A, Compare D, Angrisani D, Sanduzzi Zamparelli M, Nardone G. Alcoholic disease: liver and beyond. *World J Gastroenterol*. 2014;20:14652–9.
24. Bai X, Lu D, Liu A, Zhang Z, Li X, Zou Z, et al. Reactive oxygen species stimulates receptor activator of NF- κ B ligand expression in osteoblast. *J Biol Chem*. 2005;280:17497–506.
25. Garret IR, Boyce BF, Oreffo RO, Bonewald L, Poser J, Mundy GR. Oxygen-derived free radicals stimulate osteoclastic bone resorption in rodent bone in vitro and in vivo. *J Clin Invest*. 1990;85:632–9.
26. Enlow DH, Bang S. Growth and remodeling of the human maxilla. *Am J Orthod*. 1965;51:446–64.
27. Goldman HM, McFarlin SC, Cooper DM, Thomas CDL, Clement JG. Ontogenetic patterning of cortical bone microstructure and geometry at the human mid-shaft femur. *Anat Rec (Hoboken)*. 2009;292:48–64.
28. Sivaraj KK, Adams RH. Blood vessel formation and function in bone. *Development*. 2016;143:2706–15.
29. Greenlee DM, Dunnell RC. Identification of fragmentary bone from the Pacific. *J Archaeol Sci*. 2010;37:957–70.
30. Pries AR, Reglin B, Secomb TW. Remodeling of blood vessels: responses of diameter and wall thickness to hemodynamic and metabolic stimuli. *Hypertension*. 2005;46:725–31.
31. Palaparthi R, Saini BK, Gulati A. Modulation of diaspirin crosslinked hemoglobin induced systemic and regional hemodynamic response by ethanol in normal rats. *Life Sci*. 2001;68:1383–94.
32. Radek KA, Kovacs EJ, Gallo RL, DiPietro LA. Acute alcohol exposure disrupts VEGF receptor cell signaling in endothelial cells. *Am J Physiol Heart Circ Physiol*. 2008;295:H174–84.
33. Zhong Z, Ramsresh VK, Rehman H, Liu Q, Theruvath TP, Krishnasamy Y, et al. Acute alcohol causes hepatic mitochondrial depolarization in mice: role of ethanol metabolism. *PLoS ONE*. 2014;9:e91308.
34. Nilsson I, Rolny C, Wu Y, Pytowski B, Hicklin D, Alitalo K, et al. Vascular endothelial growth factor receptor-3 in hypoxia-induced vascular development. *FASEB J*. 2004;18:1507–15.
35. Mercer KE, Wynne RA, Lazarenko OP, Lumpkin CK, Hogue WR, Suva LJ, et al. Vitamin D supplementation protects against bone loss associated with chronic alcohol administration in female mice. *J Pharmacol Exp Ther*. 2012;343:401–12.
36. Trevisiol CH, Turner RT, Pfaff JE, Hunter JC, Menagh PJ, Hardin K, et al. Impaired osteoinduction in a rat model for chronic alcohol abuse. *Bone*. 2007;41:175–80.
37. Wezeman FH, Emanuele MA, Emanuele NV, Moskal SF 2nd, Woods M, Suri M, et al. Chronic alcohol consumption during male rat adolescence impairs skeletal development through effects on osteoblast gene expression, bone mineral density, and bone strength. *Alcohol Clin Exp Res*. 1999;23:1534–42.
38. Turner RT, Kidder LS, Kennedy A, Evans GL, Sibonga JD. Moderate alcohol consumption suppresses bone turnover in adult female rats. *J Bone Miner Res*. 2001;16:589–94.
39. Maddalozzo GF, Turner RT, Edwards CH, Howe KS, Widrick JJ, Rosen CJ, et al. Alcohol alters whole body composition, inhibits bone formation, and increases bone marrow adiposity in rats. *Osteoporos Int*. 2009;20:1529–38.
40. Maurel DB, Boisseau N, Benhamou CL, Jaffre C. Alcohol and bone: review of dose effects and mechanisms. *Osteoporos Int*. 2012;23:1–16.
41. Turner RT, Rosen CJ, Iwaniec UT. Effects of alcohol on skeletal response to growth hormone in hypophysectomized rats. *Bone*. 2010;46:806–12.
42. Cirmanová V, Bayer M, Stárka L, Zajicková K. The effect of leptin on bone—an evolving concept of action. *Physiol Res*. 2008;57:S143–51.
43. García-Valdecasas-Campelo E, González-Reimers E, Santoria-Fernández F, De la Vega-Prieto MJ, Milena-Abril A, Sánchez-Pérez MJ, et al. Serum osteoprotegerin and RANKL levels in chronic alcoholic liver disease. *Alcohol Alcohol*. 2006;41:261–6.
44. Malik P, Gasser RW, Kemmler G, Moncayo R, Finkenstedt G, Kurz M, et al. Low bone mineral density and impaired bone metabolism in young alcoholic patients without liver cirrhosis: a cross-sectional study. *Alcohol Clin Exp Res*. 2009;33:375–81.
45. Schnitzler CM, Mesquita JM, Shires R. Cortical and trabecular bone microarchitecture and turnover in alcohol-induced chronic pancreatitis: a histomorphometric study. *J Bone Miner Metab*. 2010;28:456–67.
46. Martiniaková M, Grosskopf B, Omelka R, Vondráková M, Bauerová M. Differences among species in compact bone tissue microstructure of mammalian skeleton: use of a discriminant function analysis for species identification. *J Forensic Sci*. 2006;51:1235–9.
47. Kelepouris N, Harper KD, Gannon F, Kaplan FS, Haddad JG. Severe osteoporosis in men. *Ann Intern Med*. 1995;123:452–60.